

# Role of $\sigma$ exchange in the $\gamma p \rightarrow \phi p$ process and scaling with the $f_1$ axial vector meson from a Reggeized model

Byung-Geel Yu,<sup>\*</sup> Hungchong Kim, and Kook-Jin Kong<sup>†</sup>

*Research Institute of Basic Science, Korea Aerospace University, Goyang, 412-791, Korea*

We investigate the role driven by the scalar meson  $\sigma$  exchange in the photoproduction of the vector meson  $\phi(1020)$  off a proton by using a Reggeized model. Based on the  $\pi^0(135) + \sigma(500) + f_2(1270)$ +Pomeron exchanges, we demonstrate that the  $\sigma$  exchange plays the role to reproduce the bump structure at the forward angle in the differential cross section as well as the peaking behavior in the total cross section observed in the CLAS Collaboration. We also discuss the possible observation of the scaled cross section  $s^7 d\sigma/dt$  at the production angle  $\theta = 90^\circ$  from the CLAS data. It is found that the axial vector meson  $f_1(1285)$  exchange with the trajectory  $\alpha_{f_1}(t) = 0.028t + 0.9 \pm 0.2$  arising from the axial anomaly of the QCD vacuum plays the role to clarify the scaling up to 5 GeV.

PACS numbers: 11.55.Jy, 13.40.-f, 13.60.Le

Keywords:  $\phi$  vector meson, photoproduction, scaling, scalar meson, axial vector meson

Photoproduction of the neutral vector meson has been an important tool to explore QCD dynamics via the hadronic process. Especially, the diffractive feature of the reaction process showing at high energies has drawn attention for decades, and such a nonmesonic  $t$ -channel peripheral process is, to date, materialized by the Pomeron exchange [1].

Among the light vector mesons, the  $\phi$  meson photoproduction off the proton target is special because the physical  $\phi$  meson is a pure  $|s\bar{s}\rangle$  state, whereas such a strange-quark content is hidden in the sea of the target proton. Therefore, in contrast to the cases of  $\rho^0$  and  $\omega$ , little contribution is expected from meson and baryon exchanges to the  $\phi$  meson photoproduction. In Ref. [2], one can find more discussion on how to evaluate the strangeness component in the proton contributing to the reaction process.

In this respect, the results of the recent experiments by the LEPS [3] and CLAS [4] Collaborations are interesting because a bump structure is observed in the differential cross section  $d\sigma/dt$  around  $E_\gamma \approx 2$  GeV (see Fig. 3), which cannot be expected from the monotonic behavior of the simple Pomeron-exchange model. Moreover, as the author pointed out in Ref. [5], such a bump structure gradually disappears as the scattering angle increases from the forward to the mid-angle  $\theta \approx 90^\circ$ . Of course, one might immediately suspect the nondiffractive subprocesses by the  $\pi$  and  $\eta$  exchanges in this region, but their contributions are not enough to play the role. In previous works on this issue, there were a few theoretical attempts to account for the appearance of the bump structure by including a nucleon resonance [6], or the  $K^+\Lambda(1520)$  coupled channel [7, 8] on the basis of  $\pi$ ,  $\eta$ , and the Pomeron exchanges.

In this work, motivated by the issue still open yet, we reexamine the  $\gamma p \rightarrow \phi p$  process with a focus on finding

other possibilities to explain the bump structure near threshold. Based on the well-established result in the high energy realm where the Pomeron exchange provides the diffraction in the  $t$ -channel and the exchange of the tensor meson  $f_2$  gives the long-range contribution up to  $\sqrt{s} \approx 10$  GeV, we here investigate the role of the scalar  $\sigma$  exchange in addition to the  $\pi$  exchange for the description of the reaction process near the threshold. In existing model calculations, the former exchange is usually excluded mainly because of the large uncertainty in determining its coupling strength. Nevertheless, we recall that the role of the  $\sigma$  exchange is crucial to agree with the peak of the total cross section observed in the  $\gamma p \rightarrow \rho^0 p$  process [9]. Furthermore, from the well-known aspect that the natural parity exchange would dominate the process of vector meson photoproduction, it is desirable to consider the  $\sigma$  exchange in the presence of the  $\pi$  exchange, in particular, in the low energy region.

With this in mind, we discuss the possibility of the bump structure driven by the  $\sigma$  exchange in the  $\gamma p \rightarrow \phi p$  process. Differential and total cross sections are analyzed for this purpose. Meanwhile, it is known that as the reaction energy increases, the cross section for hadron interactions shows the scaling as a manifestation of the quark structure of the hadron [10]. In our previous study on the  $\gamma p \rightarrow \pi^0 p$  process, we discussed such an energy independence of the cross section at the large transverse momentum transfer or alternatively at the mid-angle  $\theta = 90^\circ$  [11]. Likewise, we may well expect the scaling in the scaled differential cross section,  $s^7 d\sigma/dt$ , for the  $\gamma p \rightarrow \phi p$  process at the mid-angle in connection with the recent CLAS data [4]. The scaled differential cross section is composed of three parts: the resonance region where the cross section is governed by hadronic degrees of freedom, the scaling region in which quark and gluon degrees of freedom are mainly involved, and the transition region lying between them. Therefore, it will be interesting to see at what energies the quark degrees of freedom start to show up in the scaled differential cross section.

<sup>\*</sup> bgyu@kau.ac.kr

<sup>†</sup> kong@kau.ac.kr

The Reggeized amplitude for the  $\gamma p \rightarrow \phi p$  process consists of the Pomeron ( $\mathbb{P}$ ),  $f_2$ ,  $\sigma$ , and  $\pi$  exchanges which are given by

$$\mathcal{M}(\gamma p \rightarrow \phi p) = \mathcal{M}_{\mathbb{P}} + \mathcal{M}_{f_2} + \mathcal{M}_{\sigma} + \mathcal{M}_{\pi}, \quad (1)$$

where

$$\mathcal{M}_{\mathbb{P}} = 12i \frac{e \beta_q \beta_{q'}}{f_\phi} \frac{m_\phi^2}{m_\phi^2 - t} \left( \frac{2\mu_0^2}{2\mu_0^2 + m_\phi^2 - t} \right) e^{-i\frac{\pi}{2}[\alpha_{\mathbb{P}}(t)-1]} \left( \frac{s}{4s_0} \right)^{\alpha_{\mathbb{P}}(t)-1} F_1(t) \bar{u}(p') (\not{k} \eta^* \cdot \epsilon - \not{\epsilon} \eta^* \cdot k) u(p), \quad (2)$$

$$\mathcal{M}_{f_2} = \Gamma_{\gamma f_2 \phi}^{\beta \rho}(k, q) \Pi_{\beta \rho; \lambda \sigma}(Q) \bar{u}(p') \Gamma_{f_2 NN}^{\lambda \sigma}(p', p) u(p) \mathcal{R}^{f_2}(s, t), \quad (3)$$

$$\mathcal{M}_{\sigma} = \frac{g_{\gamma \sigma \phi}}{m_0} g_{\sigma NN} (k \cdot q \eta^* \cdot \epsilon - \epsilon \cdot q \eta^* \cdot k) \bar{u}(p') u(p) \mathcal{R}^{\sigma}(s, t), \quad (4)$$

$$\mathcal{M}_{\pi} = i \frac{g_{\gamma \pi \phi}}{m_0} g_{\pi NN} \varepsilon^{\mu \nu \alpha \beta} \epsilon_\mu \eta_\nu^* k_\alpha q_\beta \bar{u}(p') \gamma_5 u(p) \mathcal{R}^{\pi}(s, t), \quad (5)$$

with the Regge propagator,

$$\mathcal{R}^{\varphi}(s, t) = \frac{\pi \alpha_J' \times \text{phase}}{\Gamma[\alpha_J(t) + 1 - J] \sin[\pi \alpha_J(t)]} \left( \frac{s}{s_0} \right)^{\alpha_J(t) - J} \quad (6)$$

written collectively for the  $\varphi$  meson of spin- $J$  and  $s_0 = 1 \text{ GeV}^2$ . The phase of the  $\varphi$  is, in general, taken to be of the canonical form,  $\frac{1}{2}[(-1)^J + e^{-i\pi \alpha_J(t)}]$ , unless it is exchange-degenerate. Here,  $\epsilon(k)$  and  $\eta^*(q)$  are the photon and vector meson polarizations with the momenta  $k$  and  $q$ , respectively. Here,  $u(p)$  and  $u(p')$  are the spinors for the initial and final protons with the momenta  $p$  and  $p'$ , respectively. Here,  $Q^\mu = (q - k)^\mu$  is the  $t$ -channel momentum-transfer.

The Pomeron exchange is expressed in terms of the quark loop coupling in the  $\gamma \mathbb{P} \phi$  vertex and  $\mathbb{P} NN$  vertex with the nucleon isoscalar form factor given by [12, 13]

$$F_1(t) = \frac{4M^2 - 2.8t}{(4M^2 - t)(1 - t/0.7)^2}. \quad (7)$$

Since the Pomeron trajectory,

$$\alpha_{\mathbb{P}}(t) = 0.25t + 1.08, \quad (8)$$

as well as the physical quantities such as the decay constant  $f_\phi = -13.4$ , quark couplings  $\beta_u = \beta_d = 2.07 \text{ GeV}^{-1}$ ,  $\beta_s = 1.60 \text{ GeV}^{-1}$ , and  $\mu_0^2 = 1.1 \text{ GeV}^2$  for the quark loop in the  $\gamma \mathbb{P} \phi$  are fixed to fit to data at  $E_\gamma \geq 10 \text{ GeV}$ , we adopt these values without modification.

The tensor meson  $f_2$  exchange is expressed in terms of the radiative coupling vertex given by [14]

$$\Gamma_{\gamma f_2 \phi}^{\beta \rho}(k, q) = 4 \frac{g_{\gamma f_2 \phi}}{m_0} \times (\eta \cdot \epsilon k^\beta q^\rho + k \cdot q \epsilon^\beta \epsilon^\rho - \eta \cdot k \epsilon^\beta q^\rho - \epsilon \cdot q \eta^\beta k^\rho), \quad (9)$$

and the tensor meson-baryon vertex,

$$\Gamma_{f_2 NN}^{\lambda \sigma}(p', p) = \bar{u}(p') \left[ \frac{2g_{f_2 NN}^{(1)}}{M} (P^\lambda \gamma^\sigma + P^\sigma \gamma^\lambda) + \frac{4g_{f_2 NN}^{(2)}}{M^2} P^\lambda P^\sigma \right] u(p) \quad (10)$$

TABLE I. Listed are the physical constants and Regge trajectories with phase factors for  $\gamma p \rightarrow \phi p$ . Here,  $\varphi$  stands for  $\sigma$ ,  $\pi$ , and  $f_2$  of masses  $m_\sigma = 500$ ,  $m_\pi = 134.9766$ , and  $m_{f_2} = 1275.1 \text{ MeV}$ . For the coupling constants associated with the  $f_2 NN$  coupling, we use  $g_{f_2 NN}^{(1)} = 6.45$  and  $g_{f_2 NN}^{(2)} = 0$ .

Meson	Trajectory( $\alpha_\varphi$ )	Phase factor	$g_{\gamma \varphi \phi}$	$g_{\varphi NN}$
$\sigma$	$0.7(t - m_\sigma^2)$	$(1 + e^{-i\pi \alpha_\sigma})/2$	-0.085	14.6
$\pi$	$0.7(t - m_\pi^2)$	$e^{-i\pi \alpha_\pi}$	0.065	13.4
$f_2$	$0.9(t - m_{f_2}^2) + 2$	$(1 + e^{-i\pi \alpha_{f_2}})/2$	0.0173	6.45; 0.0

with the spin-2 projection,

$$\Pi^{\beta \rho; \lambda \sigma}(Q) = \frac{1}{2} (\bar{g}^{\beta \lambda} \bar{g}^{\rho \sigma} + \bar{g}^{\beta \sigma} \bar{g}^{\lambda \rho}) - \frac{1}{3} \bar{g}^{\beta \rho} \bar{g}^{\lambda \sigma}. \quad (11)$$

Here  $\bar{g}^{\beta \rho} = -g^{\beta \rho} + \frac{Q^\beta Q^\rho}{m_{f_2}^2}$ ,  $P^\mu = \frac{1}{2}(p' + p)^\mu$ , and  $M$  is the nucleon mass, and  $m_0 = 1 \text{ GeV}$ . The coupling constant  $g_{\gamma f_2 \phi} = 0.0173$  is determined from the partial decay width  $\Gamma_{f_2 \rightarrow \phi \gamma} = 1.3 \text{ keV}$  [15] and the tensor meson-nucleon coupling constants  $g_{f_2 NN}^{(1)} = 6.45$  and  $g_{f_2 NN}^{(2)} = 0$  are taken from Ref. [16].

For the determination of  $\gamma \sigma \phi$  coupling, it is helpful to consider the partial decay width  $\Gamma_{\phi \rightarrow \pi \pi \gamma}$ . We assume that the partial width  $\Gamma_{\phi \rightarrow \pi^0 \pi^0 \gamma} \approx 0.48 \text{ keV}$  in the Particle Data Group (PDG) is mediated by the  $\sigma$  meson and obtain  $g_{\gamma \sigma \phi} \approx 0.031$ . On the other hand, we note that Black *et al.* [17] predicted the partial width  $\Gamma_{\phi \rightarrow \sigma \gamma} = 33 \text{ keV}$  based on the vector meson dominance incorporated with the chiral effective Lagrangian. This yields  $g_{\gamma \sigma \phi} \approx 0.146$  which is somewhat larger than the naive evaluation from the  $\pi \pi \gamma$  decay width above. In the present calculation, we take the value  $g_{\gamma \sigma \phi} = 0.085$  which lies in the middle of the two extremes. The value of the  $\sigma NN$  coupling constant in the literature is very scattered and found to be in a wide range of  $5 \sim 17.9$ . We take  $g_{\sigma NN} = 14.6$  predicted by the QCD sum rule [18, 19]

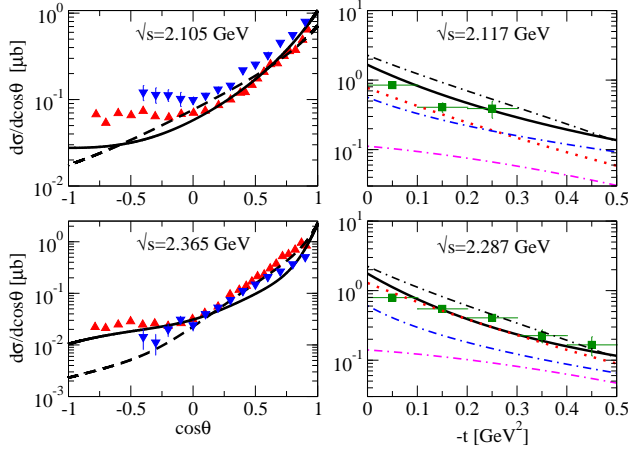


FIG. 1. Differential cross sections for  $\gamma p \rightarrow \phi p$  in the low energy region. Left panels: The black solid and dashed lines are the cross sections with and without  $\sigma$  exchange. Right panels: The contribution of each meson exchange is shown. The blue dash-dotted line is from  $\pi$  exchange, black dash-dotted line from  $\sigma$  exchange, magenta dash-dotted line from  $f_2$ , and red dotted line from the Pomeron exchange. Data at  $\sqrt{s} = 2.105$  and  $2.365$  GeV (red up triangle) are taken from the charged mode [4] and at  $\sqrt{s} = 2.13$  and  $2.38$  GeV (blue down triangle) from the neutral mode [21] in the CLAS Collaborations (left). The data in the right panel is from the LEPS data [3].

which is within the range of values from the Nijmegen soft-core NN potential model [20].

For the  $\pi$  exchange, we take the coupling constants  $g_{\pi NN}=13.4$  and  $g_{\gamma\pi\phi} = 0.065$  from the width  $\Gamma_{\phi \rightarrow \pi\gamma} = 5.42$  keV reported in the PDG. In this work, we choose the phase of  $\pi$  exchange for a better agreement with data. We summarize the coupling constants and Regge trajectories with the phase factors in Table I. In the calculation, the  $\eta$  exchange as well as the scalar mesons  $f_0$  and  $a_0$ , axial meson  $a_1$ , and tensor meson  $a_2$  are neglected for simplicity because they appear in a minor role.

In Fig. 1, we present the differential cross sections for the  $\gamma p \rightarrow \phi p$  process resulting from the coupling constants and phases in Table I. The role of the  $\sigma$  exchange is illustrated in the CLAS data, and the contribution from each meson exchange is shown in the LEPS data.

Figure 2 shows the energy dependence of the cross section from threshold up to the realm of the Pomeron exchange. The data points near the threshold are obtained by integrating out the data on the differential cross sections of Ref. [4]. As shown in the figure, there exists an inconsistency of the old measurements [22, 23] with the recent CLAS experiment [4]. Our result with the  $\sigma$  exchange as indicated by the black solid line agrees with the CLAS data, whereas the result without it favors the old data as depicted by the black dashed line. Thus, the cross section in the presence of the  $\sigma$  exchange shows the feature quite contrasting to most existing models. Indeed, in our model, the  $\sigma$  exchange is dominant near the threshold and, thus, plays the nontrivial role to make the

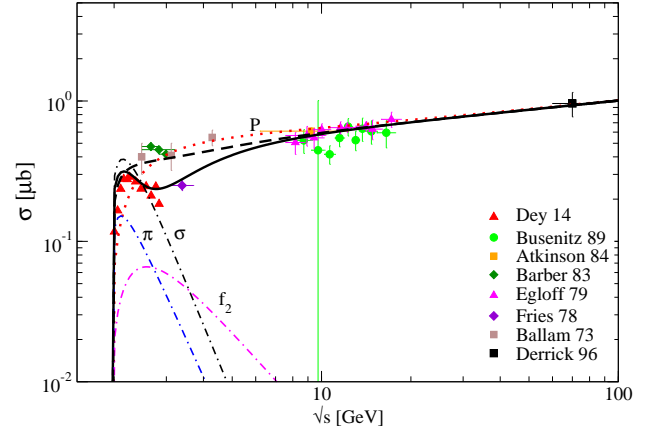


FIG. 2. Total cross section for  $\gamma p \rightarrow \phi p$  from threshold to  $\sqrt{s} = 100$  GeV. Data are taken from Refs. [4, 22–28], where the data points named as Dey 14 are obtained by integrating over the differential cross sections given in Ref. [4]. Our model favors the CLAS data [4] and data of Ref. [28] as well. Notations for the curves are the same as in Fig. 1.

small peak around  $\sqrt{s} \simeq 2.2$  GeV.

The role of the  $\sigma$  exchange in the peaking behavior of the cross section can be seen in other observables as well. Figure 3 shows the dependence of the differential cross section on the invariant energy  $\sqrt{s}$  at two different angles of  $\phi$  production in the c. m. frame. Without the  $\sigma$  exchange, the differential cross section in Fig. 3

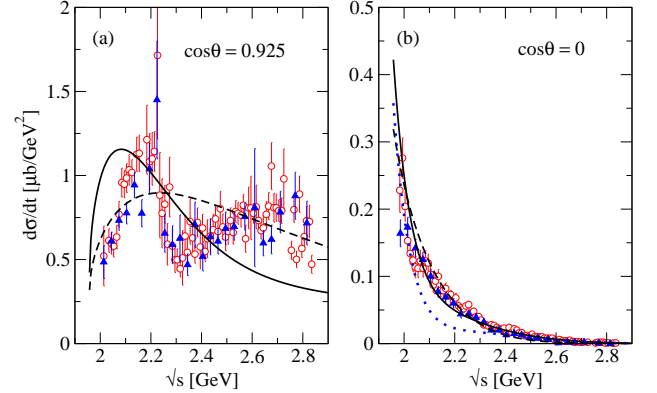


FIG. 3. Energy dependence of the differential cross sections for  $\gamma p \rightarrow \phi p$  at the production angles  $\theta = 22.33^\circ$  (a) and  $\theta = 90^\circ$  (b) in the c. m. frame. The prediction of the present model given by the solid line in (a) shows the role of the  $\sigma$  exchange in the observed peak at  $\sqrt{s} \simeq 2.2$  GeV at the forward angle in comparison to the black dashed line without the  $\sigma$  exchange. In (b), we show the dependence of the cross section on the phase of the Regge pole at the angle  $\theta = 90^\circ$ . The blue dotted line results from the  $\sigma$ ,  $\pi$ , and  $f_2$  with all canonical phases chosen. The solid and dashed lines are with and without the  $\sigma$  exchange, respectively, while the complex phase is taken for the  $\pi$  exchange. Data are from Ref. [5].

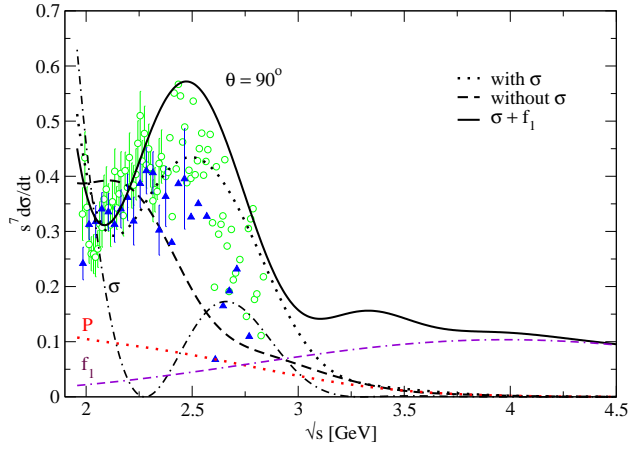


FIG. 4. Scaled differential cross sections  $s^7 \frac{d\sigma}{dt} (10^7 \text{ GeV}^{12} \text{ nb})$  for  $\gamma p \rightarrow \phi p$ . The dotted and dashed lines result from the calculation with and without the  $\sigma$  exchange, respectively, to exhibit its role crucial to form the bump at  $\sqrt{s} \simeq 2.5$  with the rapid drop following before scaling begins. The solid and dotted lines are from with and without  $f_1$  in addition to the  $\sigma$  exchange to show that its role is substantial to manifest the scaling from  $\sqrt{s} \simeq 3$  to about 5 GeV. Here,  $g_{\gamma f_1 \phi} = 0.18$ , the nucleon axial charge  $m_A = 1.08$  GeV, and  $\alpha_{f_1}(0) = 0.9$ . The contributions of the relevant meson exchanges are denoted in the figure legends. Data points at  $\theta = 90^\circ$  are obtained from Ref. [5].

(a) describes nothing but the behavior passing through the average value of data in the given energy range as shown by the dashed line. In Fig. 3(b), we illustrate the dependence of the differential cross section on the phases of the Regge poles  $\sigma$ ,  $\pi$ , and  $f_2$  at  $\theta = 90^\circ$ . It should be noted that the cross section with the canonical phases,  $(1 + e^{-i\pi\alpha})/2$  for the  $\sigma$  and  $f_2$ , and the complex phase,  $e^{-i\pi\alpha_\pi}$  for the  $\pi$  exchange, agrees with the experimental data, whereas the result with the canonical phases for all the mesons shows considerable disagreement.

Finally, let us discuss the possibility of observing the scaling in the present process at the mid-angle. Brodsky *et al.* [10] predicted that the photoproduction cross section obeys the power-law scaling, i.e.,

$$s^{n-2} \frac{d\sigma}{dt} \sim F(t_0/s), \quad (12)$$

for fixed  $t_0$  based on the quark-counting rule. Here,  $n = 9$  is the number of constituents (gauge boson plus the quarks) participating in the  $\gamma p \rightarrow \phi p$  process. The measured cross section is thus expected to exhibit such a scaling behavior as  $s^7 d\sigma/dt \sim \text{constant}$  at the fixed angle around  $\theta = 90^\circ$  (or fixed  $t_0$ ) as energy increases.

Shown in Fig. 4 is the scaled differential cross section for  $\gamma p \rightarrow \phi p$ . The data showed the bump structure around  $\sqrt{s} \simeq 2.5$  GeV with a rapid drop following. Two important points should be indicated in advance: the formation of the bump by the  $\sigma$  exchange before  $\sqrt{s} \simeq 3$  GeV and the manifestation of the nonzero scaling by the  $f_1$  exchange above 3 GeV. From the dotted and

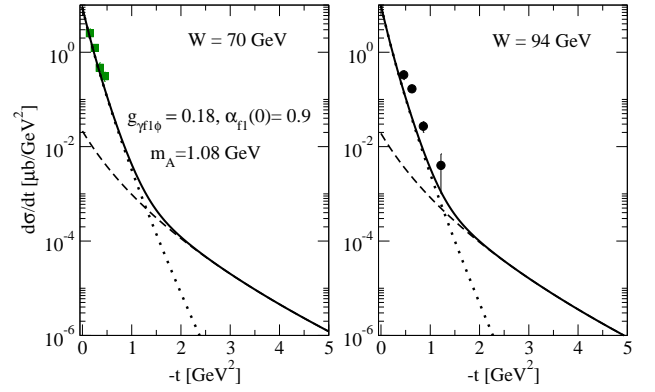


FIG. 5. Role of  $f_1$  in the differential cross sections  $\frac{d\sigma}{dt}$  at high energies. Solid and dotted lines are the calculation with and without  $f_1$  exchange, respectively. The dashed line shows the contribution of the  $f_1$  exchange. The role of  $f_1$  is apparent in the large  $-t$  with  $\alpha_{f_1}(0) = 0.9$  with respect to Ref. [29]. Data are from Refs. [24, 31].

dashed lines for the scaled cross sections with and without the  $\sigma$  exchange, the role of the  $\sigma$  exchange is crucial to drive such a bump structure with the nodes around  $\sqrt{s} \simeq 2.3$  and 3.3 GeV which are given by the vanishing of the canonical phase, i.e.,  $1 + e^{-i\pi\alpha_\sigma(t)} = 0$ , and hence,  $\alpha_\sigma(t) = -1, -3$ , and so on. Nevertheless, the scaled cross section from the exchanges of  $\sigma + \pi + f_2 + \mathbb{P}$  approaches a vanishing limit, and the energy independence of the cross section is not clear as shown by the dotted line.

In order for the scaled cross section to manifest itself as being a nonzero constant over the high energy region, interactions from the quark-gluon dynamics are expected to contribute.

In Ref. [29], a new trajectory  $\alpha_{f_1}(t) = 0.028t + (0.9 \pm 0.2)$  is suggested for the axial vector meson  $f_1(1285)$  of  $1^{++}$  by relating the properties of  $f_1$  with the two-gluon exchange via the axial anomaly of the QCD vacuum. By considering the role of the  $f_1$  peculiar to the large  $-t$  and energy, we calculate the contribution of the  $f_1$  exchange with its role expected in a larger  $-t$ , i.e., a wider range of the angle, as the energy increases. Over the region  $\sqrt{s} \simeq 3$  GeV, we obtain the scaling apparent to sustain the energy independence up to 5 GeV due to the  $f_1$  exchange which is given by [29]

$$\mathcal{M}_{f_1} = i \frac{g_{\gamma f_1 \phi}}{m_0^2} m_\phi^2 \epsilon_{\mu\nu\alpha\beta} k^\mu \eta^\nu \epsilon^\alpha (-g^{\beta\lambda} + Q^\beta Q^\lambda / m_{f_1}^2) \times \left( \frac{1}{1 - t/m_A^2} \right)^2 g_{f_1 NN} \bar{u}(p') \gamma_\lambda \gamma_5 u(p) \mathcal{R}^{f_1}(s, t). \quad (13)$$

We use the canonical phase  $(-1 + e^{-i\pi\alpha_{f_1}(t)})/2$  and the trajectory  $\alpha_{f_1}(t) = 0.028t + 0.9$  which is within the range of the intercept given in Ref. [29]. The cutoff mass  $m_A = 1.08$  GeV is chosen for the nucleon axial form factor [30] with  $g_{f_1 NN} = 2.5$ , and  $g_{\gamma f_1 \phi} = 0.18$  taken from the decay width  $\Gamma_{f_1 \rightarrow \phi\gamma} = 0.019$  MeV reported in the PDG. In practice, the physical quantities are applied to the differential cross section in parallel with the scaled

cross section to cross-check the validity of those quantities for both observables. The size of the cross section  $s^7 d\sigma/dt \approx 0.1$  [ $10^7$  GeV<sup>12</sup>nb] thus determined is consistent with the differential cross sections as shown in Fig. 5. It should also be remarked that the contribution of the  $f_1$  exchange is insignificant to other observables and could not alter much the results we have shown above.

The limitation of the Regge trajectory on such a large angle as discussed in Ref. [11] is extended by the inclusion of the  $f_1$  exchange, and our results show some evidence of the special role of the  $f_1$  axial meson as advertised in Ref. [29]. Such a scaling obtained by the  $f_1$  meson exchange in this photoproduction of  $\phi$  is quite in contrast with the scaling-violating oscillatory behavior seen in the proton-proton elastic scattering at a fixed angle [32]. In this sense, it is anticipated from future experiments to see whether the scaling persists in photoproduction of the  $\phi$  vector meson. We hope that there should be a measurement in the region above 2.8 GeV in future experiments.

It is interesting to compare the present result with that from the  $s^{12}$ -like scaling for the  $\gamma p \rightarrow \phi p$  process in Ref. [33] where the number of gluons in the hadrons and photon are counted more to give  $n = 14$ . The difference of the counting numbers between the present work and Ref. [33] leads to the different energy region expected to scale; i.e., the expected energy region the scaling appearing in Ref. [33] is below  $\sqrt{s} \simeq 3$  GeV, whereas our model predicts the scaling to start above 3 GeV.

In summary, we investigated the  $\gamma p \rightarrow \phi p$  reaction process with our interest in the possible role of the  $\sigma$  exchange as the natural parity in the low energy region. Total, differential, and the scaled cross sections are reproduced by the  $\sigma + \pi + f_2$  Regge poles on the basis of the background contribution from the Pomeron exchange up to  $\sqrt{s} = 100$  GeV. The role of the  $\sigma$  exchange in addition to the  $\pi$ ,  $f_2$ , and the Pomeron exchanges is illustrated to account for the small peak near the threshold in the to-

tal cross section and the bump structure apparent in the differential as well as the scaled differential cross section. In this respect, the  $\sigma$  exchange is an important ingredient to understand the production mechanism through the successful description of the observables we have demonstrated in the present work.

With its role in the large  $-t$  and energy by the new trajectory arising from the axial-charge distribution of the QCD vacuum, the exchange of the axial vector meson  $f_1$  is exploited to clarify the scaling above  $\sqrt{s} \simeq 3$  GeV in the scaled cross section. In that region, where quarks and gluons are expected to be involved, the result is positive to our expectation, i.e., the QCD effect through the exchange of the  $f_1$  trajectory specialized to the QCD vacuum via the axial anomaly.

Viewed from the possibility of different powers of  $s^{n-2}$  as well as the special role of the  $f_1$  related to the QCD vacuum via the axial anomaly, these findings in the scaling, in particular, would deserve focus on the high-energy photon-beam experiment to explore the quark-gluon dynamics in future experiments, such as the LEPS2 at SPring-8 and CLAS12 planned at JLab.

## ACKNOWLEDGMENTS

The work of B.-G. Yu was supported by Basic Science Research Program through the National Research Foundation of Korea(NRF) funded by the Ministry of Education, Science and Technology(NRF-2013R1A1A2010504). The work of H. Kim was supported by Basic Science Research Program through the National Research Foundation of Korea(NRF) funded by the Ministry of Education(Grant No. 2015R1D1A1A01059529).

- 
- [1] J.-M. Laget, Phys. Lett. B **489**, 313 (2000).
  - [2] A. I. Titov, Y. S. Oh, S. N. Yang, and T. Morii, Phys. Rev. C **58**, 2429 (1998).
  - [3] T. Mibe *et al.* (LEPS Collaboration), Phys. Rev. Lett. **95**, 182001 (2005).
  - [4] B. Dey *et al.* (CLAS Collaboration), Phys. Rev. C **89**, 055208 (2014).
  - [5] B. Dey, arXiv:1403.3730.
  - [6] A. Kiswandhi and S. N. Yang, Phys. Rev. C **86**, 015203 (2012).
  - [7] S. Ozaki, A. Hosaka, H. Nagahiro, and O. Scholten, Phys. Rev. C **80**, 035201 (2009).
  - [8] H.-Y. Ryu, A. I. Titov, A. Hosaka, and H.-Ch. Kim, Prog. Theor. Exp. Phys. **2014**, 023D03 (2014).
  - [9] Y. Oh, J. Korean Phys. Soc. **43**, S20 (2003).
  - [10] S. J. Brodsky and G. R. Farrar, Phys. Rev. Lett. **31**, 1153 (1973).
  - [11] K. J. Kong, T. K. Choi and B.-G. Yu, Phys. Rev. C **94**, 025202 (2016).
  - [12] A. Donnachie and P.V. Landshoff, Phys. Lett. B **478**, 146 (2000).
  - [13] Y.-S. Oh and T.-S. H. Lee, Phys. Rev. C **69**, 025201 (2004).
  - [14] P. Singer, Phys. Rev. D **27**, 2223 (1983).
  - [15] S. Ishida and K. Yamada, Phys. Rev. D **40**, 1497 (1989).
  - [16] B. G. Yu, T. K. Choi, and W. Kim, Phys. Lett. B **701**, 332 (2011).
  - [17] D. Black, M. Harada, and J. Schechter, Phys. Rev. Lett. **88**, 181603 (2002).
  - [18] G. Erkol, R. G. E. Timmermans, and T. A. Rijken, Phys. Rev. C **72**, 035209 (2005).
  - [19] G. Erkol, R. G. E. Timmermans, M. Oka, and Th. A. Rijken, Phys. Rev. C **73**, 044009 (2006).
  - [20] M. M. Nagels, T. A. Rijken, and J. J. de Swart, Phys. Rev. D **17**, 768 (1978).
  - [21] H. Seraydaryan *et al.* (CLAS Collaboration), Phys. Rev. C **89**, 055206 (2014).
  - [22] D. P. Barber *et al.*, Z. Phys. C **12**, 1 (1982).

- [23] J. Ballam *et al.*, Phys. Rev. D **7**, 3150 (1973).
- [24] M. Derrick *et al.*, Phys. Lett. B **377**, 259 (1996).
- [25] J. Busenitz *et al.*, Phys. Rev. D **40**, 1 (1989).
- [26] M. Atkinson *et al.*, Nucl. Phys. **B231**, 15 (1984).
- [27] R. M. Egloff *et al.*, Phys. Rev. Lett. **43**, 657 (1979).
- [28] D. C. Fries, P. Heine, H. Hirschmann, A. Markou, E. Seitz, H.-J. Behrend, W. P. Hesse, W. A. McNeely, and T. Miyachi, Nucl. Phys. **B143**, 408 (1978).
- [29] N. I. Kochelev, D. P. Min, Y. Oh, V. Vento, and A. V. Vinnikov, Phys. Rev. D **61**, 094008 (2000).
- [30] A. Liesenfeld *et. al.*, Phys. Lett. B **468**, 20 (1999).
- [31] J. Breitweg *et. al.*, Eur. Phys. J. C **14**, 213 (2000).
- [32] B. Pire and J. P. Ralston, Phys. Lett. B **117**, 233 (1982).
- [33] B. Dey, Phys. Rev. D **90**, 014013 (2014).